

A MODEL TO ESTIMATE CO₂ LEAKAGE AND IDENTIFY CO₂ HYDRATE STABLE CONDITIONS FOR OFFSHORE CCS

Hariharan Ramachandran^{1*}

¹ CAGE - Centre for Arctic Gas Hydrate, Environment and Climate, Department of Geosciences, UiT-The Arctic University of Norway, Tromsø, Norway

* Corresponding author e-mail: hariharan.r@uit.no

Abstract

Offshore CCS (Carbon Capture and Storage) is an attractive option to clamp down on carbon emissions. Two major advantages are 1) existing infrastructure for injection and 2) well characterized reservoirs due to previous oil and gas operations. One of the biggest concerns is the possibility of leakage. Leakage is likely when CO₂ plume encounters improperly abandoned wellbores, pre-existing conductive faults, or reactivated faults amongst others. The hazard of leakage strongly depends on the leakage fluxes and rates. Hydrates may form and throttle leakage if the pressure-temperature conditions within the pathway reach hydrate stable conditions. Thus, a useful component of risk assessment is to model CO₂ leakage and assess potential for hydrate formation conditions. In this short paper, we describe a model for flow of CO₂ along a leakage pathway. We assume single phase flow of CO₂ with variable fluid properties and a continuous leakage pathway with constant thickness. These assumptions help obtain worst-case estimates of leakage fluxes and rates. Expected leakage fluxes and rates are estimated along with the effect of pathway permeability and reservoir overpressure on it. Pressure-temperature conditions are checked if they fall within the CO₂ hydrate stable conditions for typical Norwegian Continental Shelf (NCS) Storage projects (Sleipner, Snøhvit and Aurora projects). Formed hydrates reduce the permeability of the pathway and has the potential to temporarily block leakage or redirect leakage in different directions. The aim of this study is to understand the relationship between pathway properties, regional conditions, leakage pressure profile and hydrate formation on leakage fluxes and rates.

Keywords: CO₂ leakage; Hydrates; Offshore CCS; Modeling; Leakage risk; Leakage flux

1. Introduction

Global effort has been undertaken with the announcement of Paris agreement to limit the average temperature rise to 2 °C and CO₂ concentration to 450 ppm by the end of the 21st century [1][2]. One key suggestion to clamp down on carbon emissions is to add the Carbon Capture and Storage (CCS) for existing and new fossil-fuel based power sources and other energy intensive industries [3]. Captured CO₂ is transported and injected in deep geological formations. In some sense, CCS is the process of returning carbon to where it was produced from, albeit in an altered form [4]. Previous studies [5] have shown that large volumes of CO₂ can be stored in aquifers by dissolution, trapping and mineralization. The most considered storage formations [6] are depleted oil and gas fields [7], deep saline aquifers [8] and unminable coal seams [8][9]. Depleted oil and gas reservoirs are especially an attractive option because of existing infrastructure and well characterized storage formation.

One of the biggest risks associated with storage is the possibility of leakage [6][10]. CO₂ may escape (Refer Figure 1) through man-made pathways, such as poorly completed and/or abandoned wells pre-dating storage operations [11][12], or through pre-existing or reactivated faults/fractures [13]. Besides providing a direct release of leaking CO₂ at seafloor/surface, they also spread them at shallower depths with a possibility to contaminate [6][10][14]. This provides a motivation to analyze the leakage along such pathways. A good physics-based model to predict leakage characteristics

will be helpful during the site selection phase from risk assessment perspective [15].

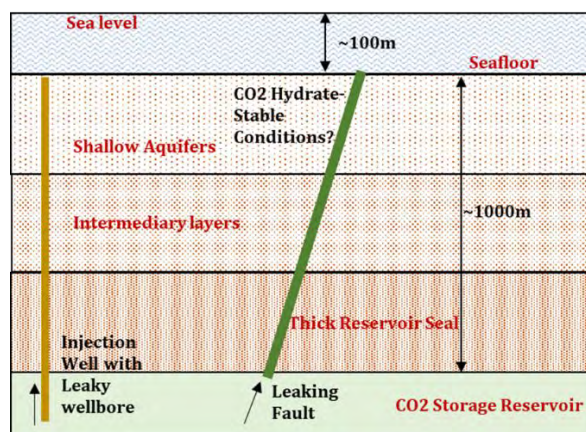


Figure 1: Schematic representation of offshore leakage scenario. CO₂ leaks through a fault or wells with leaky wellbore. The leakage pathway terminates at the seafloor. Does CO₂ encounter hydrate-stable conditions as it reaches the seafloor?

Understanding the pressure and temperature conditions occurring during leakage and its implications on CO₂ properties is critical for modeling leakage [20][21][22]. CO₂ is in supercritical state at typical storage conditions. The temperature and pressure profile of a vertical fault at hydrostatic and geothermal equilibrium is shown on a CO₂ phase diagram in Figure 2. The seafloor depth and reservoir depth are taken from Figure 1. Pressure and temperature decrease from the leakage source to the

seafloor. The key observation from Figure 2 is that CO₂ can exist in different phases during leakage. Since the pressure and temperature decrease continuously, there will be a substantial variation in CO₂ properties such as density, viscosity etc. This decompressive nature will also affect the pressure profile within the fault [20][21][22]. It's instructive to check if the new pressures reach hydrate stable conditions. Accounting for above factors is critical in getting a good leakage estimate.

Several studies have developed analytical and semi-analytical models to estimate leakage fluxes [16][17][18][19] through faults and wellbores. The fluxes were estimated with an isothermal assumption mostly (non-isothermal assumption was used in certain section of the pathway [19]) and issues related to the permeability of the pathways and the pressure at the leakage source were well addressed. The non-isothermal nature of leakage throughout the pathway and multiphase coexistence considerations (condensation, evaporation, and hydrate formation) were studied extensively too [20][21][22][23].

In this study, we present a simplified steady state model to predict leakage fluxes and rates in non-isothermal and hydrate stable conditions. The simplified approach help predict the worst-case fluxes when leakage occurs. This model is used to predict leakage for wide variety of pathway geological properties and regional constraints such as geothermal gradients. This model can also assess if hydrate stable conditions exist during leakage.

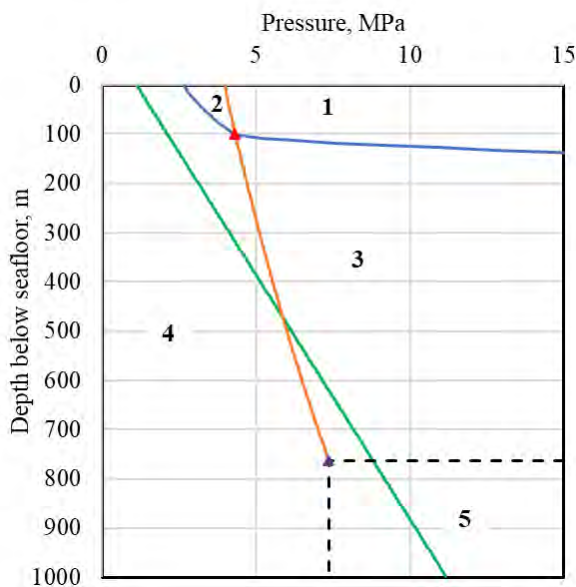


Figure 2: Typical pressure-temperature profile for a slow leaking fault (green line) shown in Figure 1. This profile is superimposed on the phase diagram of CO₂. Orange line is the Saturation line for CO₂ and purple triangle is the critical point. Gas and liquid phase coexist in this pressure-temperature condition. Region 3 has liquid phase and region 4 has gas phase. CO₂ exists in supercritical conditions in region 5. The hydrate forming conditions for CO₂-H₂O mixtures is shown by the blue curve and the red triangle is the quadruple point. CO₂ hydrate exists in region 1 and 2.

2. Methods

The simplified steady-state flow model is presented in this section. A leakage pathway is assumed to intersect the storage reservoir. The injected CO₂ is assumed to have reached the base of the leakage pathway and 100% CO₂ is assumed to leak. The leakage pathway is a generic term. It refers to faults under high permeability and leaky wellbore under low permeability [19]. Analysis for other types of leakage pathways can be performed by altering the pathway properties in this model [21][23]. The pathway is assumed to be a 1-D vertical porous medium with specific geometry (effective width, breadth), rock properties (porosity, permeability) and rock-fluid properties (relative permeability, initial saturations). The complexities related to the geology of fault core / leaky wellbore and the damaged zone surrounding it is simplified. Averaged values were used along the horizontal directions, but they can vary with depth. Complex pathway characteristics related to in-situ stress, stress-dependent properties, fracture branching amongst other geomechanical factors are not included in this model. The aqueous phase is assumed to be at residual saturation. This assumption is intended to calculate the worst-case fluxes when leakages occur.

Summary of the assumptions used to derive the mass balance are:

- 1) Steady state 1-D flow of CO₂ in the vertical pathway.
- 2) Constant pressure and temperature at the bottom and top of the pathway.
- 3) Multiphase Darcy's law is applied to flow in pathway.
- 4) Capillary pressure is neglected.
- 5) Residual water saturation in pathway after steady state flow of CO₂ reached.
- 6) Hydrates will only affect the permeability in the formed region.
- 7) The temperature in the pathway is assumed to have equilibrated with the geothermal temperature

The overall mass balance constraint equation is given as,

$$\frac{dm}{dz} = 0 \quad 2-1$$

The multiphase flowing effects are ignored and only CO₂ (in gas, liquid, or supercritical conditions) can flow and assumed to establish steady saturation. The flow rate is,

$$\dot{m} = -\frac{\rho_j k k_{rj} A}{\mu_j} \left(\frac{dP}{dz} - \rho_j g \right) \quad 2-2$$

Where m is the total mass rate, A is the area perpendicular to flow, k is the absolute permeability of the pathway, k_{rj} is the relative permeability of phase j , μ_j is the viscosity of phase j and ρ_j is the mass density of phase j . Hydrate formation is assumed to affect the permeability alone. Several experiments [24][25] have been reported showing the effect of CO₂-hydrates on rock permeability and calibrated the correlation between the permeability and hydrate saturation as,

$$k_{new} = (1 - S_h)^{n_h} k \quad 2-3$$

The new permeability, k_{new} in the hydrate region is only a function of the hydrate saturation, S_h , and a hydrate exponent, n_h . An exponent of 3 was used for this study based on the experimental results [24][25]. The CO₂ hydrate stable pressures for a given temperatures and seawater salinity conditions were published [26] and a correlation was developed using this data,

$$P_{hyd} = \sum_{i=0}^7 A_i T^i \quad 2-4$$

Table 1: Constant Values for Equation 2-4

Constant	If T ≤ 281.58K	If T > 281.58K
A ₀	-1.4022673445909542 * 10 ¹⁰	+2.252510579962195 * 10 ¹²
A ₁	+3.5856298042175686 * 10 ⁸	-4.738766839485371 * 10 ¹⁰
A ₂	-3.9292771701155193 * 10 ⁶	+4.1538268190587914 * 10 ⁸
A ₃	+2.392087196483884 * 10 ⁴	-1.9418959119972903 * 10 ⁶
A ₄	-87.37405622572473	+5106.4822557848065
A ₅	+0.1914826448303001	-7.16163577830236
A ₆	-2.331279266183065 * 10 ⁻⁴	+4.184920304845536 * 10 ⁻³
A ₇	+1.2163909288497183 * 10 ⁻⁷	0.0

P_{hyd} is the hydrate stable pressure in MPa for the given temperature, T in K and A_i is equation constants given in Table 1. It is assumed that all the water (with seawater salinity) available is converted to hydrates when the pressure-temperature condition is hydrate stable. This is a reasonable assumption for low water saturations. CO₂ properties vary along the pathway as both temperature and pressure vary with depth. Span-Wagner multi-parameter Equation Of State for CO₂ [27] is employed for phase behavior and fluid properties estimation and a corresponding state model for viscosity [38][39]. The pressure at the seafloor is given as,

$$P_{sf} = P_{atm} + D_{sf} * HG \quad 2-5$$

P_{sf} is the pressure at the seafloor in MPa, D_{sf} is the seafloor depth, P_{atm} is the atmospheric pressure taken as 0.101325 MPa and HG is the hydrostatic gradient in MPa/m. The temperature and pressure below the seafloor are given as,

$$T = T_{sf} + D * GG \quad 2-6$$

$$P = P_{sf} + D * HG \quad 2-7$$

T_{sf} is the seafloor temperature in K, D is the sediment depth below seafloor in m and GG is the geothermal gradient in K/m. The mass flux and pressures are the unknowns that are solved for using the model. The mass balance equation (2-1) together with mass flux equation (2-2 and 2-3) is solved to obtain the leakage flux. The pathway is discretized into blocks and the equations are solved iteratively until the mass balance constraint is

honored. The temperature within the blocks is determined using equation (2-6) and the pressure boundary conditions are determined using equation (2-5 and 2-7) This model is coded in Julia [33].

3. Results

3.1 Base Case

This section discusses a synthetic base case for the model. A homogenous vertical pathway from the seafloor to a depth of 1000 mbsf (meters below seafloor) with a permeability of 1 Darcy is considered. The cross-sectional area allowable for flow is kept constant. The seafloor depth, seafloor temperature and geothermal gradient typical for Norwegian Continental Shelf (NCS) were obtained from previous studies [28]. The initial pathway pressure is described by the hydrostatic gradient. The bottom of the pathway is assumed to be connected to a continuous source of CO₂ at constant pressure and temperature. The storage reservoir is overpressurized due to the injection and storage (Overpressure, $\Delta P_s = P_{reservoir} - P_{hydrostatic}$). An overpressure of 2 MPa is assumed. The pathway is assumed to be at residual water saturation of 0.2 and constant gas relative permeability of 0.8. The geological description is shown in Table 2 and schematic representation is shown in Figure 3.

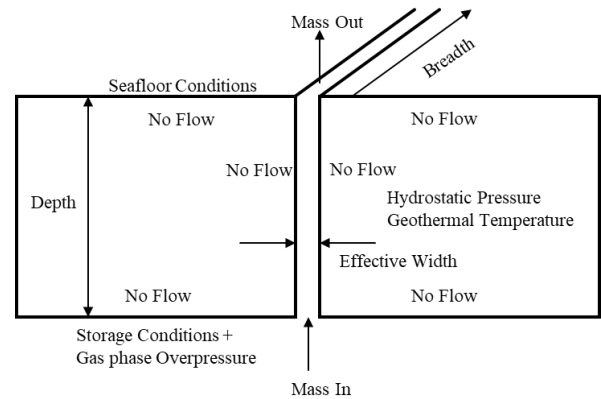


Figure 3: Schematic representation of leakage pathway system used for synthetic base case to represent NCS.

Table 2: Input parameters for synthetic base case

Geological Description	Values
Pathway porosity, ϕ	0.3
Pathway effective width (m), w	0.1
Pathway permeability (D), k	1.0
Pathway breadth (m), b	10.0
Pathway depth (mbsf), D	1000.0
Initial Conditions	
Seafloor depth (m), D_{sf}	100.0
Seafloor temperature (K), T_{sf}	278.15
Geothermal gradient (K/m), GG	0.034
Hydrostatic gradient (MPa/m), HG	0.01
Overpressure at leakage source (MPa), ΔP_s	2.0
Pressure at seafloor (MPa), P_{sf}	1.008
Pressure at leakage source (MPa), P	13.16
Temperature at leakage source (K), T	312.065

The resulting pressure-temperature profiles within the pathway at the onset of leakage is shown in Figure 4. The pressure in the pathway is higher than the corresponding hydrostatic pressure at every depth but lower than the hydrate-stable pressure for the given temperature conditions. Although this might provide a driving force for CO₂ to leak-off from the pathway into intersecting permeable layers if any, higher pressures will provide a signal to nearby observation wells during monitoring phase which may lead to quicker remediation.

The leakage flux is calculated to be 0.044 kg/s/m² or 1399.2 ton/year/m². For the sake of comparison, leakage flux from an isothermal model is calculated to be 0.066 kg/s/m² or 2100.9 ton/year/m². Calculations for the isothermal model are performed with density and viscosity of CO₂ averaged between leakage source conditions and seafloor conditions. The results indicated that the isothermal model overestimated leakage flux by 50% compared with current model. Direct consequences of such overestimation are 1) the risk associated with leakage is overestimated affecting the site selection process and 2) the leakage pathway properties such as permeability is underestimated from the obtained monitoring data [23].

The leakage flux is expressed independent of the area. Assuming 1 m² of leakage area, the leakage rate is approximately 1,399.2 ton/year. This result is sensitive to the area of the pathway and to attenuation to intersecting permeable layers among other factors. Both these factors affect the final leakage rate. In the context of long-term risk assessment, this leakage rate for 100 years would yield 0.14 million tons of escaped CO₂, approximated to 0.7% for a 20 million tons storage project, well below the 1% target [6]. The fluxes estimated by the model report the worst-case fluxes and not necessarily the real-world scenario.

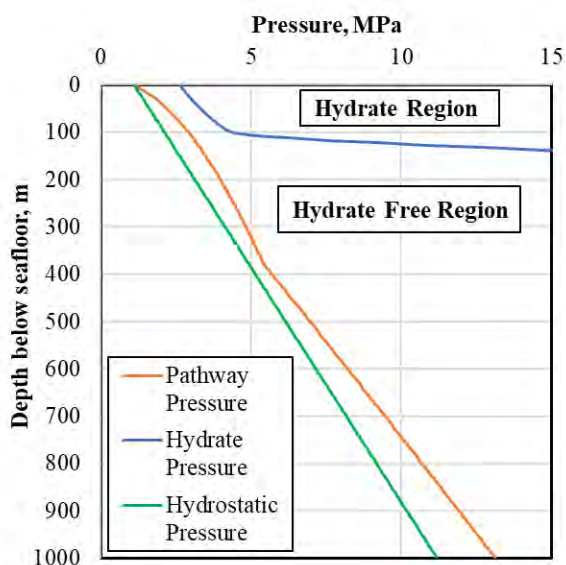


Figure 4: Pressure profile with depth for synthetic base case. The pathway pressure is in the single-phase regions and don't reach hydrate formation conditions.

3.2 Effect of Permeability

Leakage flux increased in a log-linear fashion with the increase in permeability as shown in Figure 5. A sensitivity study was performed on permeability to estimate its effect on leakage flux keeping all other parameters same as the base case. The variation in permeability does not affect the fluid properties. For an order of magnitude permeability increase, the leakage flux increased by a factor of 10. For comparison, the CO₂ background flux at earth's surface is 0.2 mg/s/m² [29]. The intention here is to set the calculated fluxes in context with background fluxes and not to comment on whether the values are large or small enough to neglect when compared. This provides confidence that the leaks can be easily identified during monitoring for permeability greater than 10 μD.

Flux through leaky faults are quite high with a possibility for runaway discharge and compromise the storage operation. Leakage fluxes are around 0.1 ton/year/m² for 0.0001 Darcy pathway signifying typical leaky wellbore [12][19]. Assuming 1 m² of leakage area, 15,000 leaky wellbores need to be encountered to reach 1% leakage over 100 years for a 20 million tons storage project and the above leakage flux. From overall leakage perspective, leaky wellbores provide less of risk than leaky faults. In the context of long-term risk assessment, all the wellbores/faults and other pathways in contact with the reservoir needs to be accounted for. Specifically, whether they are leaky or not and their permeability distribution.

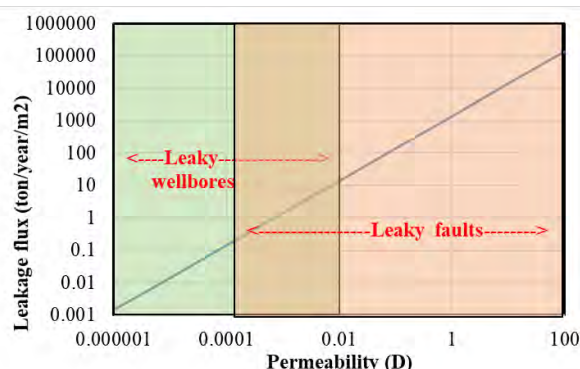


Figure 5: Leakage rate as function of permeability. Green region is typical permeability reported [12][19] for leaky wellbores and red region reported [21] for leaky faults.

3.3 Effect of Overpressure

The CO₂ storage reservoir is typically at hydrostatic pressure. The pressure in the reservoir increases during injection assuming no production or leakage. The increase in pressure above hydrostatic is referred to as overpressure. CO₂ typically occupies the top of the reservoir, and the length of this connected CO₂ phase is attributed to an increase in pressure. Typical pressure profiles within a reservoir are discussed in previous studies [19][20][23]. A simplified version of this effect is used here as constant overpressure in all our simulations. A sensitivity study was performed on overpressure to estimate its effect on leakage flux keeping all other parameters same as the base case. Leakage flux increases

with increase in overpressure as shown in Figure 6. Besides the concerns with respect to the unintended fracturing, higher rate of injection will increase the overpressure and the leakage flux. It is preferable to inject slower and longer than faster and shorter when concerned about minimizing the leakage flux. Thus, reservoir pressure management plays an active role in minimizing leakage.

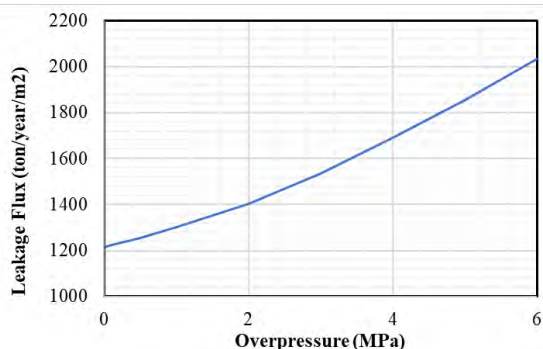


Figure 6: Leakage flux as function of constant reservoir overpressure.

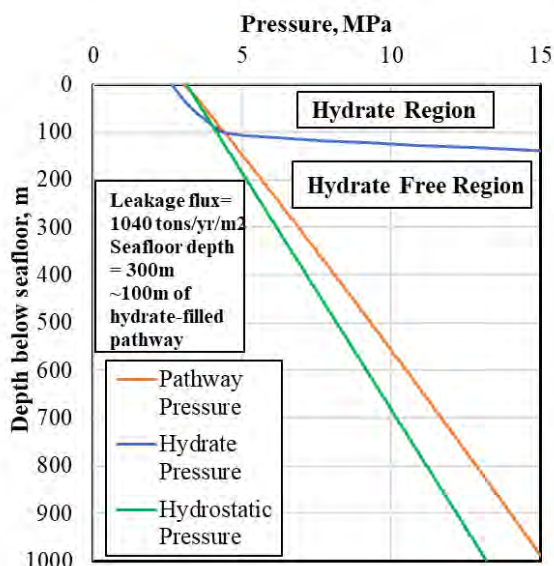


Figure 7: Pressure profile with depth for base case with a different seafloor depth of 300m. Close to 100m of CO₂-hydrate filled zone is present in the pathway

3.4 CO₂- Hydrate Stable Conditions

Pressures within the pathway for base case conditions (Figure 3) was far away from hydrate stable conditions. But it is instructive to find out what conditions facilitate hydrate formation within the pathways. Increase in reservoir depth, colder conditions (low geothermal gradient) and larger overpressure conditions were not found to assist hydrate formation. On analysis, two factors strongly assisted hydrate formation. They were colder seafloor temperatures and greater seafloor depths as shown in Figure 7 and Figure 8. Amount of aqueous phase present will determine the hydrate saturation within this region. Over time, there is potential for formed hydrates to accumulate enough to block pathways

as observed in marine methane seeps, gas chimneys and active pockmarks [30] [31][32]. Formed hydrates act as a signal during the shallow subsurface monitoring phase. Recent studies show even a minor change in gas or hydrate saturation could be detected using the time-lapse seismic approach [37].

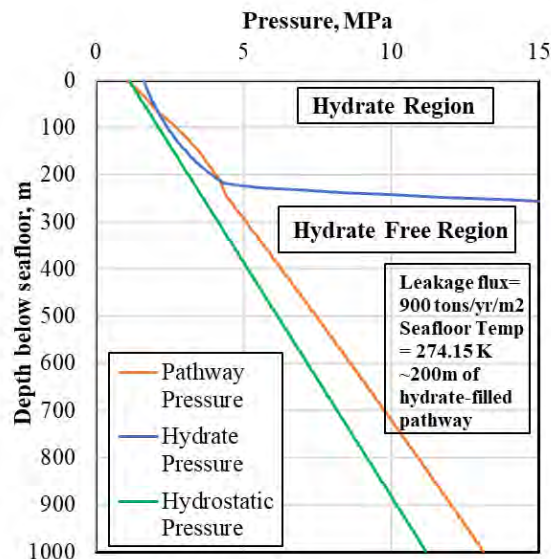


Figure 8: Pressure profile with depth for base case with different seafloor temperature of 274.15K. Close to 200m of CO₂-hydrate filled zone is present in the pathway.

3.5 Leakage Analysis for Storage Sites in NCS

Hypothetical leakage scenario from CCS projects (Sleipner project, Snøhvit project and Aurora/ Northern Lights project) in Norwegian Continental Shelf (NCS) is analyzed in this section and the corresponding data is shown in Table 3 [28][34][35][36]. The maximum uncertainty is on the seafloor temperature and geothermal gradient. From previous section, geothermal gradient was found to have minimal impact when compared with seafloor temperature on leakage pathway reaching CO₂ hydrate stable conditions.

Table 3: Input parameters for hypothetical leakage analysis on real field information [28][34][35][36].

Geological Description	Sleipner	Snøhvit	Aurora
Pathway porosity, ϕ	0.3		
Pathway effective width (m)	0.1		
Pathway permeability (D)	1		
Pathway breadth (m)	10		
Initial Conditions	Sleipner	Snøhvit	Aurora
Seafloor depth (m)	80	330	300
Seafloor temperature (K)	278.15	277.15	276.15
Geothermal gradient (K/m)	0.034	0.035	0.036
Overpressure at leak source (MPa)	2		
Pathway depth (m)	700	2600	2700

The pressure conditions in the pathway along with CO₂ hydrate stable pressure and hydrostatic pressure is shown in Figure 9 (for Sleipner project), Figure 10 (for Snøhvit

project) and Figure 11 (for Aurora project). The pathway pressure is far away from hydrate stable conditions for the Sleipner project, but they reach CO₂ hydrate stable conditions in the upper 150m for the Snøhvit and Aurora project. Although there are considerable uncertainties here, the results indicate that in the event of leakage, it is very likely for hydrates to form at the Snøhvit and Aurora projects they might temporarily block the pathways [30][31][32]. The leakage fluxes were considerably lower for Snøhvit and Aurora project (~900 ton/year/m²) when compared with Sleipner project (~1500 ton/year/m²). Larger seafloor depth (> 300 m) coupled with colder seafloor temperatures (< 277 K) were found to be amenable for CO₂ hydrate formation along the pathway during leakage.

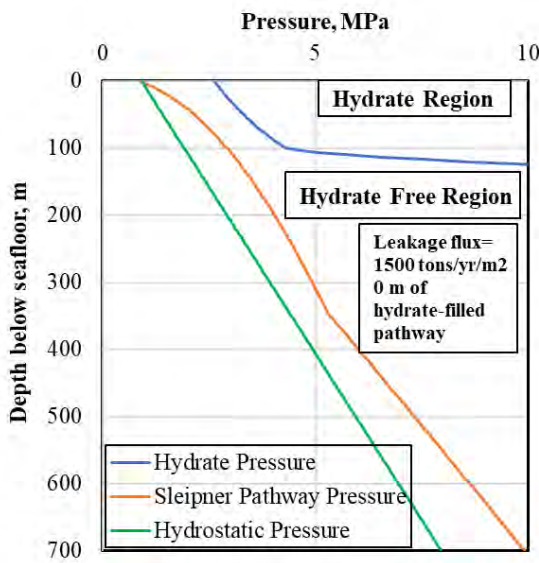


Figure 9: Pressure profile with depth for Sleipner project. No CO₂-hydrates are present in the pathway.

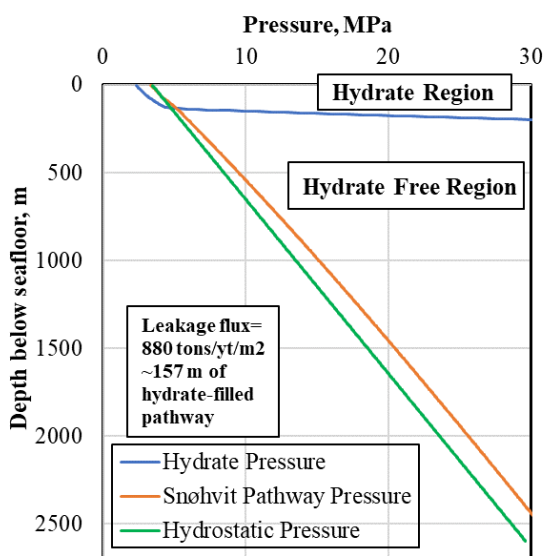


Figure 10: Pressure profile with depth for Snøhvit project. Close to 157m of CO₂-hydrate filled zone is present in the pathway.

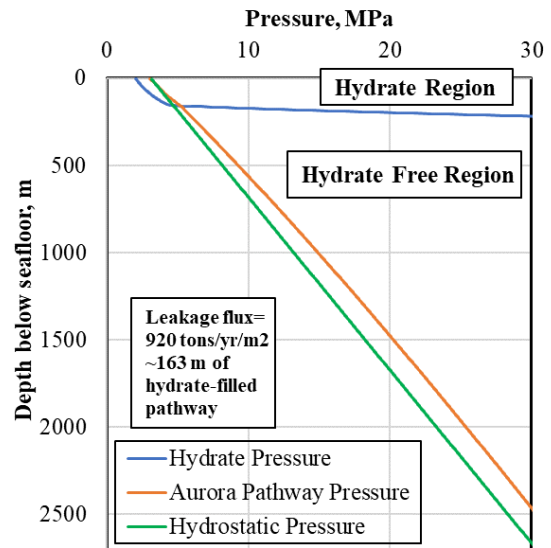


Figure 11: Pressure profile with depth for Aurora project. Close to 163m of CO₂-hydrate filled zone is present in the pathway.

4. Conclusion

The steady-state leakage model estimates leakage fluxes along all types of leakage pathway. Additionally, it has the capability to assess for hydrate stable conditions and estimate the impact of formed hydrates on permeability and leakage fluxes. This model allows quick estimation of fluxes, follows physics-based approach, and fits well into the risk assessment framework. Example calculations were shown for highly idealized representation of leakage pathway and regional conditions commonly observed in Norwegian continental shelf (to mimic offshore CCS operation).

Results indicate permeability has a first-order effect on leakage fluxes. Other factors such as overpressure affect the fluxes, but not as much as the factor of permeability. Open faults leak more than leaky wellbores. Larger seafloor depth (> 300 m) and colder seafloor temperatures (< 277 K) were found to be amenable for CO₂ hydrate formation along the pathway during leakage. Hypothetical leakage at Snøhvit and Aurora project were found to reach CO₂ hydrate stable conditions along the pathway and no hydrates at Sleipner project. Further analysis is needed to check if this may lead to potential blockages and gas chimney formation.

The leakage fluxes estimates shown here should be considered as relative values based on the idealized assumptions rather than predictions of actual values. The geometry and properties of an actual fault will be much more complex than assumed in these simple models. However, the leakage fluxes calculated using a numerical reservoir simulator with a more realistic description of a fault is a challenging task and is also subject to many uncertainties. The results in this paper indicate the importance of taking the multiphase and non-isothermal nature of leakage in such simulations.

Acknowledgements

This work was supported by the SEAMSTRESS project. SEAMSTRESS project is supported by starting grants from the Tromsø Research Foundation and the Research Council of Norway (grant nr. 2878659) awarded to Andrea Plaza-Faverola.

References

- [1] UNFCCC. (2015a). Decision 1/CP.21, in report of the conference of the parties on its twenty-first session, held in Paris from 30 November to 13 December 2015. Addendum Part two: Action taken by the Conference of the Parties at its twenty-first session (FCCC/CP/2015/10/Add.1).
- [2] UNFCCC. (2015b). Synthesis report on the aggregate effect of the intended nationally determined contributions (FCCC/CP/2015/7).
- [3] Leung, D. Y., Caramanna, G., & Maroto-Valer, M. M. (2014). An overview of current status of carbon dioxide capture and storage technologies. *Renewable and Sustainable Energy Reviews*, 39, 426-443.
- [4] RISCs, (2014). A Guide to Potential Impacts of Leakage from CO₂ Storage. *British Geological Survey*, 70.
- [5] Kumar, A., Noh, M. H., Ozah, R. C., Pope, G. A., Bryant, S. L., Sepehrmoori, K., & Lake, L. W. (2005). Reservoir Simulation of CO₂ Storage in Aquifers. *SPE Journal*, 10(03), 336-348.
- [6] IPCC (Intergovernmental Panel on Climate Change), (2005). Special Report on Carbon Dioxide Capture and Storage. Cambridge University Press, Cambridge, UK, New York, NY, USA.
- [7] Stevens, S. H., Kuuskraa, V. A., Gale, J. and Beecy, D. (2001), CO₂ Injection and Sequestration in Depleted Oil and Gas Fields and Deep Coal Seams: Worldwide Potential and Costs. *Environmental Geosciences*, 8: 200–209.
- [8] White, C.M., Strazisar, B.R., Granite, E.J., Hoffman, J.S. and Pennline, H.W., 2003. Separation and capture of CO₂ from large stationary sources and sequestration in geological formations—coalbeds and deep saline aquifers. *Journal of the Air & Waste Management Association*, 53(6), pp.645-715.
- [9] Reeves, S.R. and Schoeling, L., 2001. Geological sequestration of CO₂ in coal seams: reservoir mechanisms field performance, and economics.
- [10] Jimenez, J.A. and Chalaturnyk, R.J., 2003, January. Are Disused Hydrocarbon Reservoirs Safe for Geological Storage of CO₂? In *Greenhouse Gas Control Technologies-6th International Conference* (pp. 471-476). Pergamon.
- [11] Gasda, S.E., Bachu, S. and Celia, M.A., 2004. Spatial characterization of the location of potentially leaky wells penetrating a deep saline aquifer in a mature sedimentary basin. *Environmental geology*, 46(6-7), pp.707-720.
- [12] Tao, Q. and Bryant, S.L., 2014. Well permeability estimation and CO₂ leakage rates. *International Journal of Greenhouse Gas Control*, 22, pp.77-87.
- [13] Rutqvist, J., Birkholzer, J., Cappa, F. and Tsang, C.F., 2007. Estimating maximum sustainable injection pressure during geological sequestration of CO₂ using coupled fluid flow and geomechanical fault-slip analysis. *Energy Conversion and Management*, 48(6), pp.1798-1807.
- [14] Jones, D.G., Beaubien, S.E., Blackford, J.C., Foekema, E.M., Lions, J., De Vittor, C., West, J.M., Widdicombe, S., Hauton, C. and Queirós, A.M., 2015. Developments since 2005 in understanding potential environmental impacts of CO₂ leakage from geological storage. *International Journal of Greenhouse Gas Control*, 40, pp.350-377.
- [15] Pawar, R.J., Bromhal, G.S., Carey, J.W., Foxall, W., Korre, A., Ringrose, P.S., Tucker, O., Watson, M.N. and White, J.A., 2015. Recent advances in risk assessment and risk management of geologic CO₂ storage. *International Journal of Greenhouse Gas Control*, 40, pp.292-311.
- [16] Celia, M.A., Bachu, S., Nordbotten, J.M., Gasda, S.E. and Dahle, H.K., 2005. Quantitative estimation of CO₂ leakage from geological storage: Analytical models, numerical models, and data needs. In *Greenhouse Gas Control Technologies 7* (pp. 663-671). Elsevier Science Ltd.
- [17] Nordbotten, J.M., Celia, M.A. and Bachu, S., 2005. Injection and storage of CO₂ in deep saline aquifers: analytical solution for CO₂ plume evolution during injection. *Transport in Porous media*, 58(3), pp.339-360.
- [18] Chang, K.W., Minkoff, S.E. and Bryant, S.L., 2009. Simplified model for CO₂ leakage and its attenuation due to geological structures. *Energy Procedia*, 1(1), pp.3453-3460.
- [19] Tao, Q., Checkai, D., Huerta, N. and Bryant, S.L., 2011. An improved model to forecast CO₂ leakage rates along a wellbore. *Energy Procedia*, 4, pp.5385-5391.
- [20] Pruess, K., 2004. Numerical simulation of CO₂ leakage from a geologic disposal reservoir, including transitions from super- to subcritical conditions, and boiling of liquid CO₂. *Spe Journal*, 9(02), pp.237-248.
- [21] Ramachandran, H., Pope, G.A. and Srinivasan, S., 2014. Effect of thermodynamic phase changes on CO₂ leakage. *Energy Procedia*, 63, pp.3735-3745.
- [22] Ramachandran, H., Pope, G.A. and Srinivasan, S., 2017. Numerical Study on the Effect of Thermodynamic Phase Changes on CO₂ Leakage. *Energy Procedia*, 114, pp.3528-3536.
- [23] Ramachandran, H., 2017. Modeling CO₂ leakage through faults and fractures from subsurface storage sites (Doctoral dissertation).
- [24] Kumar, A., Maini, B., Bishnoi, P.R., Clarke, M., Zatepina, O. and Srinivasan, S., 2010. Experimental determination of permeability in the presence of hydrates and its effect on the dissociation characteristics of gas hydrates in porous media. *Journal of petroleum science and engineering*, 70(1-2), pp.114-122.
- [25] Masuda, Y., 1997. Numerical calculation of gas production performance from reservoirs containing natural gas hydrates. In *Annual Technical Conference, Soc. of Petrol. Eng., San Antonio, Tex., Oct. 1997*.
- [26] Duan, Z. and Sun, R., 2006. A model to predict phase equilibrium of CH₄ and CO₂ clathrate hydrate in aqueous electrolyte solutions. *American Mineralogist*, 91(8-9), pp.1346-1354.
- [27] Span, R. and Wagner, W., 2003. Equations of state for technical applications. III. Results for polar fluids. *International Journal of Thermophysics*, 24(1), pp.111-162.
- [28] Allen, R., Nilsen, H.M., Lie, K.A., Møyner, O. and Andersen, O., 2018. Using simplified methods to explore the impact of parameter uncertainty on CO₂ storage estimates with application to the Norwegian Continental

- Shelf. *International Journal of Greenhouse Gas Control*, 75, pp.198-213.
- [29] Allis, R., Bergfeld, D., Moore, J., McClure, K., Morgan, C., Chidsey, T., Heath, J. and McPherson, B., 2005, May. Implications of results from CO₂ flux surveys over known CO₂ systems for long-term monitoring. In Fourth annual conference on carbon capture and sequestration, DOE/NETL.
- [30] Plaza-Faverola, A., Bünz, S., Johnson, J.E., Chand, S., Knies, J., Mienert, J. and Franek, P., 2015. Role of tectonic stress in seepage evolution along the gas hydrate charged Vestnesa Ridge, Fram Strait. *Geophysical Research Letters*, 42(3), pp.733-742.
- [31] Bünz, S., Polyakov, S., Vadakkepuliambatta, S., Consolaro, C. and Mienert, J., 2012. Active gas venting through hydrate-bearing sediments on the Vestnesa Ridge, offshore W-Svalbard. *Marine Geology*, 332, pp.189-197.
- [32] Daigle, H. and Dugan, B., 2010. Origin and evolution of fracture-hosted methane hydrate deposits. *Journal of Geophysical Research: Solid Earth*, 115(B11).
- [33] Bezanson, J., Edelman, A., Karpinski, S. and Shah, V.B., 2017. Julia: A fresh approach to numerical computing. *SIAM review*, 59(1), pp.65-98.
- [34] Eiken, O., Ringrose, P., Hermanrud, C., Nazarian, B., Torp, T.A. and Høier, L., 2011. Lessons learned from 14 years of CCS operations: Sleipner, In Salah and Snøhvit. *Energy Procedia*, 4, pp.5541-5548.
- [35] Tasianias, A., Mahl, L., Darcis, M., Buenz, S. and Class, H., 2016. Simulating seismic chimney structures as potential vertical migration pathways for CO₂ in the Snøhvit area, SW Barents Sea: model challenges and outcomes. *Environmental Earth Sciences*, 75(6), p.504.
- [36] Wu, L., Thorsen, R., Ottesen, S., Meneguolo, R., Hartvedt, K., Ringrose, P. and Nazarian, B., 2021. Significance of fault seal in assessing CO₂ storage capacity and containment risks—an example from the Horda Platform, northern North Sea. *Petroleum Geoscience*.
- [37] Waage, M., Singhroha, S., Bünz, S., Planke, S., Waghorn, K.A. and Bellwald, B., 2021. Feasibility of using the P-Cable high-resolution 3D seismic system in detecting and monitoring CO₂ leakage. *International Journal of Greenhouse Gas Control*, 106, p.103240.
- [38] Vesovic, V., Wakeham, W.A., Olchowy, G.A., Sengers, J.V., Watson, J.T.R. and Millat, J., 1990. The transport properties of carbon dioxide. *Journal of physical and chemical reference data*, 19(3), pp.763-808.
- [39] Fenghour, A., Wakeham, W.A. and Vesovic, V., 1998. The viscosity of carbon dioxide. *Journal of physical and chemical reference data*, 27(1), pp.31-44.